



Construction of a domestic wastewater disinfection filter from biosynthesized and commercial nanosilver: a comparative study

Heba S. Taher^{1*} , Rania Sayed², Asmaa Loutfi¹ and Hesham Abdulla¹

Abstract

Purpose: Biosynthesis of nanoparticles is an eco-friendly process and considered one of the most significant aspects of nanotechnology. Silver nanoparticles (Ag NPs) have a better bactericidal activity due to its high surface area to volume ratio. In this paper, *Streptomyces* sp. U13 (KP109813) was used to biosynthesize silver nanoparticles (Ag NPs) to construct wastewater disinfection filter.

Methods: The biosynthesized nanosilver and a commercially available ink nanosilver were characterized, and their wastewater disinfection efficiency was compared. The nanometrological characteristics of both nanosilver such as structure, shape, and size were investigated using the X-ray diffraction (XRD), Fourier transform-infrared spectroscopy (FTIR), high-resolution transmission electron microscope (HR-TEM), and UV-visible spectroscopy.

Result: The results revealed that the biosynthesized and ink Ag NPs were well dispersed and had a spherical shape, with sizes ranged from 5 to 37 nm and from 2 to 26 nm, respectively. To examine the disinfection capabilities, Ag NPs were loaded on two substrates, foam and limestone gravel, and packed into a glass column receiving domestic wastewater. Results showed that Ag NPs attached to limestone gravel eliminate 100% of the coliform bacteria better than foam. Comparing to control columns (without silver), only 50 and 10% reduction of the total coliform in gravel and foam column were achieved, respectively.

Conclusion: This work concluded that the type of substrate controls the amount of Ag NPs loaded on it and thus controls the disinfection process. No significant difference between biosynthesized and ink nanosilver in wastewater disinfection was observed. Using limestone gravel filter loaded with 200 mg/l Ag NPs with contact time of 150 min achieves a complete eradication of coliform bacteria.

Keywords: Silver nanoparticles, Nanometrological measurements, *Streptomyces*, Characteristics, Wastewater disinfection, Coliform

Introduction

Nanotechnology is an emerging and fast-growing technology. Currently, there are a huge number of nanotechnology-based products on market. Nanomaterial

is known as a natural, incidental, or manufactured material having particles, in an unbound state or as an aggregate or as an agglomerate, and where one or more of the external dimensions are in the size range 1–100 nm (Bondarenko et al. 2013). The use of nanomaterials is expanded in a wide range of applications such as energy, health, and the environment.

Among all manufactured nanomaterials, nano-sized silver is the most widely used in different applications. Silver nanoparticles (Ag NPs) possess unique

*Correspondence: heba_taher@science.suez.edu.eg

¹ Botany and Microbiology Department, Faculty of Science — Suez Canal University, Ismailia, Egypt
Full list of author information is available at the end of the article



© The Author(s) 2022. **Open Access** This article is licensed under a Creative Commons Attribution 4.0 International License, which permits use, sharing, adaptation, distribution and reproduction in any medium or format, as long as you give appropriate credit to the original author(s) and the source, provide a link to the Creative Commons licence, and indicate if changes were made. The images or other third party material in this article are included in the article's Creative Commons licence, unless indicated otherwise in a credit line to the material. If material is not included in the article's Creative Commons licence and your intended use is not permitted by statutory regulation or exceeds the permitted use, you will need to obtain permission directly from the copyright holder. To view a copy of this licence, visit <http://creativecommons.org/licenses/by/4.0/>.

physicochemical properties (Elechiguerra et al. 2005) that open a wide range of applications, one of which is water purification (Bielefeldt et al. 2009). It is mainly used to remove three major pollutants including, pesticides, heavy metals, and microorganisms (Que et al. 2018). Ag NPs are known as excellent antimicrobial agents; they could be used as alternative disinfectants in water treatment systems (Elechiguerra et al. 2005; Sayed et al. 2018).

A variety of synthesis processes have been reported for nanoparticles preparation and characterization. Physical methods are costly, and chemical methods are mostly toxic (Parisa et al. 2015). Biological methods via plants and microorganisms are promising green alternative (Jannathul and Lalitha 2015; Benakashania et al. 2016; Erico et al. 2016; Bakhtiari-Sardari et al. 2020).

Actinomycetes are gram-positive filamentous bacteria with high GC content. It is used in nanotechnology because of its unique capability to produce various bioactive component and high protein content to produce nanoparticles both intracellularly and extracellularly (Gahlawat and Choudhury 2019). Several studies proved that *Streptomyces* could synthesize Ag NPs by direct contact with mycelial mass (Tsibakhashvili et al. 2011), cell-free metabolites (Vidhyashree et al. 2015; Al-Dhabi et al. 2019; Bakhtiari-Sardari et al. 2020), or partially purified metabolite (Abou-Dobara et al. 2017).

The multiple pressures of climate change, population growth, industrialization, and urbanization have led to the declining availability of freshwater resources (Sun et al. 2016). According to the World Health Organization (WHO), more than 1.5 million children die each year due to bad sanitation (WHO (World Health Organization) 2015). Wastewater discharges in water resources are the major source of pathogens. Safe management of wastewater can yield multiple benefits; in this context, there is a real requirement for more efficient and powerful technologies for the treatment of wastewater (Ferroudj et al. 2013). Chlorination is extensively used for disinfecting sewage effluents, but by-products such as toxic organic halogen could be produced (Chu et al. 2016). Ozone requires the use of complicated equipment, while bacterial regrowth is possible after UV irradiation (Wang et al. 2015).

The ideal disinfectant should possess a broad antimicrobial spectrum within a short time, no generation of harmful by-products, low-energy cost, easy operation and easy to store, must not be corrosive, and capable of safe disposal. Silver in the form of nanoparticles that release silver ions more effectively has a better bactericidal activity due to its high surface area to volume ratio (Duran et al. 2010). Researchers deposited Ag NPs on different solid materials for wastewater treatment like sand (Mahmood et al. 1993), zeolite (Matsumura et al.

2003), fibreglass (Nangmenyi et al. 2009), silica microbeads (Quang et al. 2011), cotton, wool, and nylon fabrics (Pasricha et al. 2012), resin beads (Mthombenia et al. 2012), activated carbon (Altintig et al. 2016), foams (Altintig et al. 2016), and magnetic biochar/poly (dopamine) composite (Li et al. 2019). These reports showed that the type of substrate controls the amount of Ag NPs that are loaded on it and thus controls the disinfection process. A technical committee in the field of nanotechnology (TC 299), established by the international organization for standardization (ISO), published standards and guides related to the specification of characteristics and relevant measurement methods for silver nanoparticles that are intended for antibacterial applications in nanotechnology (ISO/TS 20660:2019).

The present study aims to the designing of a cost-effective wastewater disinfection filter that employed biosynthesized silver nanoparticles using actinomycete strain and investigating their characteristics and disinfection performance compared to commercially available silver nanoparticles.

Materials and methods

Biosynthesis of Ag NPs

Six native actinomycete strains were isolated from sandstone rock collected from Um Bogma village, Sinai, Egypt (Abdulla et al. 2018), were screened for Ag NPs synthesis. They have been recorded in GenBank with accession numbers; they are *Actinobacterium* U12 (KP109814), *Streptomyces* sp. U13 (KP109813), *Streptomyces atrovirens* U19 (KP109811), *Streptomyces* sp. U30 (KP109810), *Streptomyces humidus* UA9 (KP109809), and Actinomycetales bacterium UA15 (KP109812). Phenotypically, the six strains produced aerial mycelium on ISP4 media with colours, olive, grey, and white; also, they varied in their substrate mycelium colour. Spore suspension of the tested strains was inoculated into starch casein broth and incubated at 28 °C under continuous agitation at 100 rpm for 3 days. The biomass was harvested by centrifugation and then rinsed twice with distilled water. The washed pellets were resuspended in sterile tap water. To determine the dry weight, an aliquot of the suspension was centrifuged and dried overnight at 60 °C to a constant weight. Twenty-five milligrams dry weight equivalent of each strain was washed twice with deionized water and resuspended in 100 ml of 25 mg Ag⁺/l (as Ag NO₃); pH was adjusted to 7. This screening experiment for the biosynthesis of Ag NPs was carried out in duplicate at 28 °C overnight on 110 rpm shaking; development of brown colour was considered positive result. The suspensions were left to settle; formation of Ag NPs in biomass-free supernatant was confirmed by UV-Vis scan.

Streptomyces sp. U13 (KP109813) was selected as the most active isolate. It was examined to synthesize Ag NPs at different Ag⁺ concentrations (25, 50, 75, and 100 mg/l) and different biomass weights (20, 40, 60, 80, and 100 mg dry weight equivalent) at pH 7 while incubated overnight at 28 °C. The best conditions were selected to biosynthesize Ag NPs to be characterized and used in the wastewater disinfection experiments compared to commercially available ink Ag NPs (Sayed et al. 2018). The commercially ink Ag NPs was from Metalon; it was well dispersed in aqueous that stabilized by capping agent to be suited to inkjet printing of electronic components. The stability and homogeneity of the Ag NPs ink were the reason of choice for comparison with the biosynthesized Ag NPs.

Ag NPs characterization

Different techniques were used to study the nanometrological characteristics of the biosynthesized Ag NPs and commercially available ink Ag NPs. UV-Vis spectrophotometer (Shimadzu, UV3101PC, Japan) was used to confirm the formation of Ag NPs in solution at room temperature. The absorbance spectra were recorded from 300 to 700 nm with a 1-nm interval. The X-ray diffraction analysis (XRD) was carried out by diffractometer (D8 Advance, Bruker, Germany) with Cu-K α ($\lambda = 1.542 \text{ \AA}$) operated at 45 kV and 40 mA at room temperature. The analysis was performed in the wide-angle range from 10 to 80° with step 0.02°. The chemical structure of Ag NPs was investigated by using a Fourier transform-infrared spectrometer (FT/IR-4100 type A, JASCO, Japan). The measurements were performed at the wavenumber range from 4000 to 450 cm⁻¹ at a resolution of 0.96 cm⁻¹. High-resolution transmission electron microscopy (HR-TEM, JEOL JEM 2100, Japan) with an acceleration voltage of 200 kV was used to determine the size and shape of Ag NPs. The TEM sample was prepared by dropping the suspension of Ag NPs on a copper grid and allowed to dry at room temperature.

Wastewater disinfection experiments

Domestic wastewater samples were collected from the pre-chlorination stage from Sarabium wastewater treatment plant in Ismailia, Egypt, and were used on the same day of sampling. Disinfection was evaluated by detection of total coliform bacteria; a subsample was taken before disinfection for the initial count. Total coliform was cultured on Endobase medium (Lab M-England) after serial dilutions using pour plate technique followed by incubation at 37 °C for 24 h. The diluent was saline and was used with a dilution factor of 10⁻³ and 10⁻⁴ for initial count and 10⁻¹ and 10⁻² for control columns samples. It is worth noting that cultivation of coliform was directly without dilutions from Ag NPs loaded columns.

Coating of silver nanoparticles on substrate

Two substrates, foam and limestone gravel, were selected to carry the biosynthesized Ag NPs. The two substrates were selected due to their high surface area, low cost and availability, and difference in nature. The foam is artificial, while the limestone is natural. Two-hundred forty grams of each substrate with a diameter (6–8 mm) was washed twice by distilled water with shaking for 30 min. Washed substrates were soaked in a suspension of Ag NPs (250 ml) with a concentration of 400 mg/l on a shaker for 24 h in the dark, and then, they were removed and kept in a dark clean place to dry. Each coated substrate (240 g) was used to fill a glass column (4-cm diameter, 23-cm height), and the columns were washed with distilled water twice to remove unbound particles. To ensure the binding of Ag NPs on examined substrates, the concentrations of remnant Ag NPs after coating and washing were measured using atomic absorption spectroscopy (PerkinElmer).

Column experiment

A total of 150 ml of domestic wastewater were poured into each packed column along with a control (column with substrates without Ag NPs); the columns were conducted in duplicates. Samples were taken after 6 h to evaluate the disinfection capacity, and silver discharge was measured by atomic absorption spectroscopy.

Column experiment with different conditions

Limestone gravel was chosen as a substrate to test different disinfection conditions. These conditions were disinfection mode, nanoparticles concentration, and nanosilver type (the biosynthesized compared to commercially ink Ag NPs). Two modes were tested for the disinfection process, continuous flow mode, and static mode. In the continuous flow mode, the wastewater was run from a reservoir to the column with a flow rate of 2 ml/min. In the static mode, the wastewater was retained in the column, and a sample was taken periodically every 30 min. To evaluate different concentrations of the biosynthesized Ag NPs on the disinfection process, another set of columns was established using a concentration of 200 mg/l Ag NPs to coat gravel under static mode.

The ink Ag NPs were chosen as a commonly used synthetic Ag NPs to compare between the disinfection efficiency of the biosynthesized Ag NPs and commercially available source. The biosynthesized Ag NPs and ink Ag NPs at concentration 200 mg/l were used to coat gravel and assembled the columns (Fig. 1) as mentioned above, and the disinfection process was evaluated using static mode.

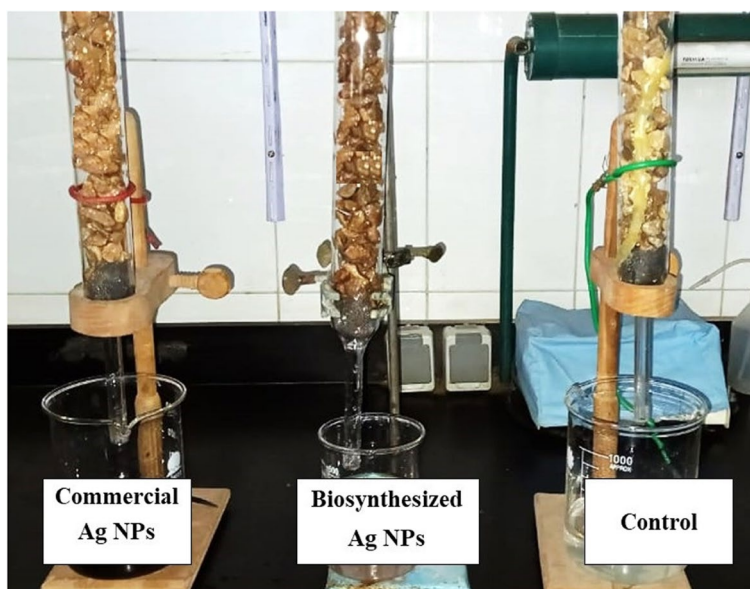


Fig. 1 Gravel columns loaded with biosynthesized and commercially ink Ag NPs in comparison to control

Results and discussion

Biosynthesis of Ag NPs

The formation of Ag NPs was observed visually by the change of solution colour from colourless to brown. *Streptomyces* sp. U13 showed a change in solution colour (Fig. 2), while in the rest strains only the biomass colour was changed to greyish brown with a slight change in colour of the solution. Extracellular formation of Ag NPs was confirmed by UV-Vis scan from 300 to 700 nm. The UV-visible spectra (Fig. 3) showed increased absorbance, and a peak was recorded at 434 nm only in the case of *Streptomyces* sp. U13. Several studies proved that several strains of *Streptomyces* synthesized Ag NPs (Vidhyashree

et al. 2015; Abou-Dobara et al. 2017; Al-Dhabi et al. 2019; Bakhtiari-Sardari et al. 2020).

Streptomyces strains can synthesize Ag NPs intracellularly and extracellularly. Although the biomass colour of the rest tested strains was changed indicating intracellular biosynthesis, only the extracellular Ag NPs were characterized. Extraction of the intracellular Ag NPs needs the application of suitable detergents or ultrasonic treatment. Economically, extracellular synthesis of Ag NPs is preferred for large-scale production because it is cheap, simple, and can be easily purified. *Streptomyces* mechanisms for reducing AgNO₃ into Ag NPs are not fully recognized. Ag NPs could be synthesized by direct

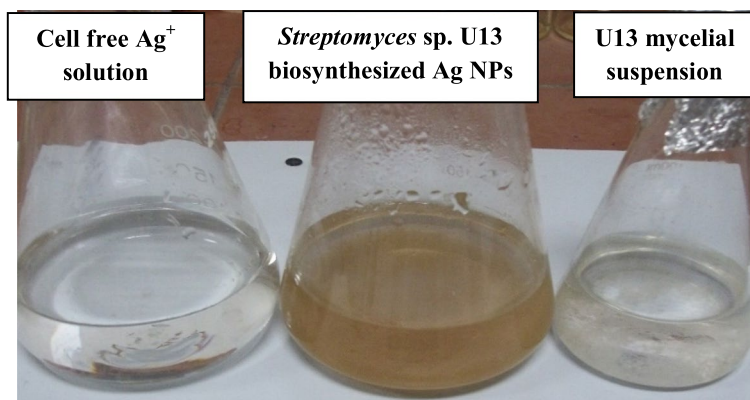


Fig. 2 Biosynthesis of Ag NPs by *Streptomyces* sp. U13 actinomycete strain showing change of colour to brown

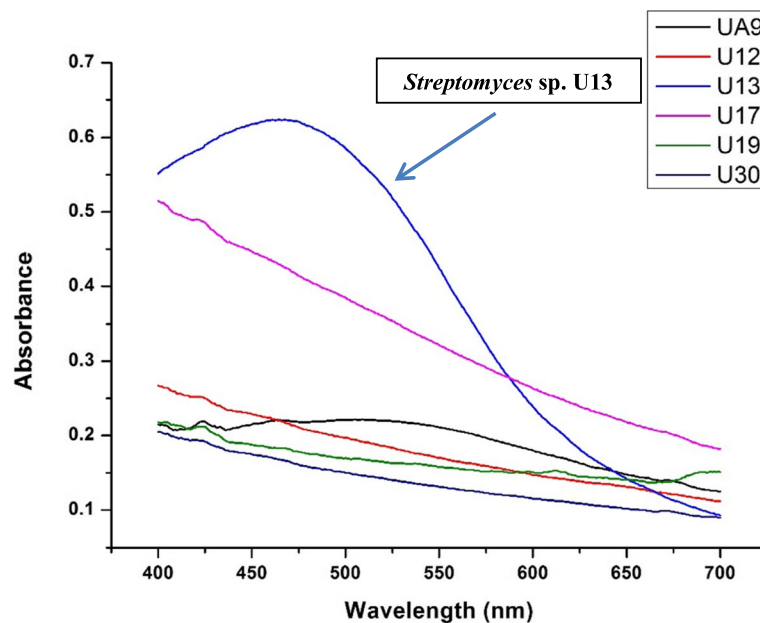


Fig. 3 UV-Vis scan of extracellular Ag NPs formed by the six tested actinomycete strains. Only *Streptomyces* sp. U13 actinomycete strain showed the characteristic absorption band of Ag NPs

contact with mycelial mass (Tsibakhashvili et al. 2011), cell-free metabolites (Vidhyashree et al. 2015; Al-Dhabi et al. 2019; Bakhtiari-Sardari et al. 2020), or partially purified metabolite (Abou-Dobara et al. 2017).

UV-Vis scan results reflect differences in Ag NPs characterization as well as in quantity. The results showed that increasing Ag^+ concentrations increased the quantity of the produced Ag NPs, as shown in Fig. 4 a and c. The colour of the solutions became darker, and the absorbance increased in spectrophotometric scanning. Using 100 mg Ag^+/l (equivalent to 1 mM AgNO_3), the highest Ag NPs concentration was obtained as shown in scan curve height (Fig. 4a). Dada et al. (2018) reported that the most appropriate and suitable concentration of AgNO_3 is 1 mM as where better surface plasmon resonance was obtained. Wagi and Ahmed (2020) found that increases in Ag NPs due to AgNO_3 increase are not the case for every strain and vary from species to species.

Increasing biomass weights is also affecting the synthesis process by increasing the produced Ag NPs quantity (Fig. 4b), but when the biomass elevated to 100 mg (dry weight equivalent), the produced Ag NPs became greyish and precipitated rapidly. The results showed that the best conditions for the synthesis of Ag NPs were 100 mg Ag^+/l and 80 mg dry weight equivalent. These conditions were selected to synthesize Ag NPs to be characterized and used in the wastewater disinfection experiments.

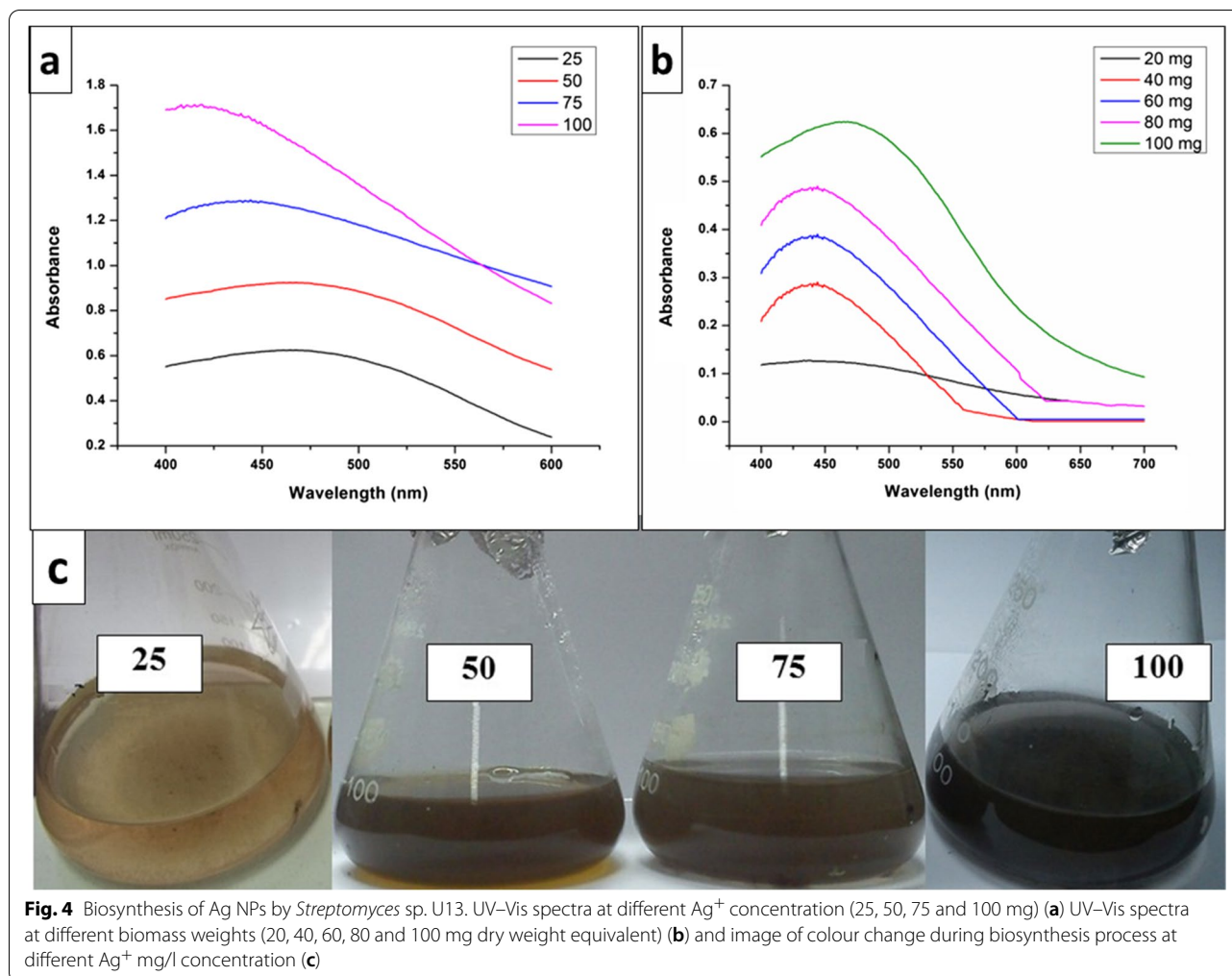
Ag NPs characterization

UV-Vis spectroscopy

The absorption band in the visible region considers the main characteristic of silver nanoparticles. Optical absorption spectra of Ag NPs are dominated by surface plasmon band which shows red end or blue end shift depends on size, shape, and aggregation of the particles (Lufsyi et al. 2015). Figure 5a showed that successfully biosynthesized silver nanoparticles, with light brown colour, had the surface plasmon absorption band with a maximum of 434 nm in the visible region. In Fig. 5b, abroad signal in the visible range with a maximum at about 414 nm was observed for commercially available synthesized silver nanoparticles (ink nanosilver) with dark brown colour due to the combined vibration of Ag NPs in resonance with the light wave (Dubey et al. 2010). The wideness of the absorption spectrum curves is a good evidence of the nanoparticle size, and the two observed absorption bands of Ag NPs indicate the presence of spherical or roughly spherical shape of particles (Guzmán et al. 2008).

X-ray diffraction studies (XRD)

The XRD pattern of biologically and commercially available synthesized silver nanoparticles was recorded in the range between 20 and 80° (2 θ), step of 0.04°, and 2 s per step. The samples for XRD analysis were prepared by using a pipette to put drops of Ag NPs solution on a



glass slide to achieve uniformly thin films. The XRD pattern of the biosynthesized Ag NPs sample was illustrated in Fig. 5c. The XRD pattern showed the Bragg's diffraction peaks of Ag NPs at 38.16° , 45.04° , and 64.75° , respectively, corresponding to (111), (200), and (220) planes of the face-centred cubic lattice. The other peak at 32.78° may be appeared due to crystallization of bioorganic phase (Sathiyar and Akilandeswari 2014; Selvi et al. 2016). These results are in good agreement with those reported in the previous literature (Phanjom and Ahmed 2015; Vasudeva et al. 2018). Figure 5d shows that the commercially available synthesized Ag NPs (ink nanosilver) are found to be amorphous. These results are in line with previous reports (Harajyoti and Ahmed 2011; Sayed et al. 2018).

Fourier transform-infrared spectroscopy analysis (FTIR)

FTIR analysis was performed for biosynthesized and commercially available Ag NPs. The biosynthesized Ag NPs shows absorption peaks at 3449.06, 2092.39,

1637.27, 1460.81, 1259.29, and 1161.9 as indicated by transmittance% in Fig. 5e. The functional groups corresponding to these absorption peaks are O–H stretching, C=O stretching, C=O stretching of amide groups of proteins, amino and amino-methyl stretching groups of protein, C–O–C stretching, and C–O stretch (Phanjom and Ahmed 2015; Vasudeva et al. 2018). The sharp absorption peak at 1637.27 cm^{-1} indicates that proteins are interacting with biosynthesized Ag NPs without affecting their secondary structure during reaction with Ag^+ ions or after binding with Ag NPs (Fayaz et al. 2010). The IR spectroscopic analysis confirms the presence of proteins acting as capping agent to prevent agglomeration of nanoparticles and provide stability to the medium (Sathiyavathi et al. 2010).

FTIR spectrum of the commercially available Ag NPs (ink nanosilver) was presented in Fig. 5f. It shows that seven peaks located at 3470.28, 2096.24, 1639.2, 1436.71, 1163.83, 1114.65, and 1039.44 cm^{-1} are assigned for

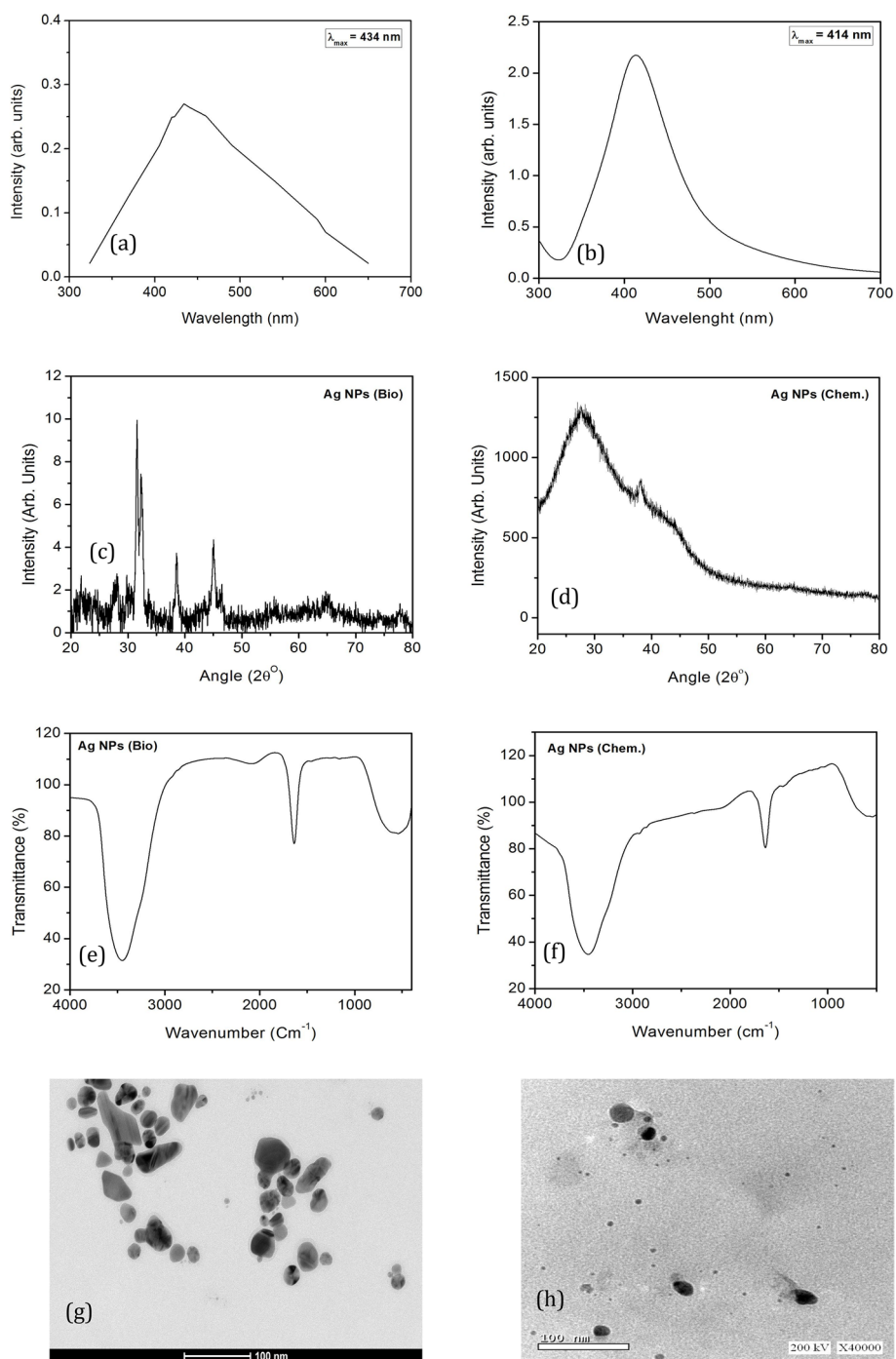


Fig. 5 Characteristics of silver nanoparticles. UV-Vis spectra of biosynthesized Ag NPs (a), UV-Vis spectra of commercially available Ag NPs (ink Ag NPs) (b), XRD pattern of biosynthesized Ag NPs (c), XRD spectra of ink Ag NPs (d), FTIR spectra of biosynthesized Ag NPs (e), FTIR spectra of ink Ag NPs (f), TEM image of biosynthesized Ag NPs (g), and TEM image of ink Ag NPs (h)

O–H, C≡C, C=C, N–H, C–O, C–O, and C–N stretch vibration mode, respectively. The same results were reported in previous literature (Preetha et al. 2013; Kumari et al. 2016).

High-resolution transmission electron microscope (HR-TEM) ISO 21363:2020 (nanotechnologies — measurements of particle size and shape distributions by transmission electron microscope) has been published recently

by the international organization for standardization (ISO) to study the morphology of nanoparticles. The size and shape of the two samples of silver nanoparticles were obtained by using the nanometrological technique HR-TEM. The samples were prepared by dropping the Ag NPs solution onto a micro copper grid. TEM images in Fig. 5g and h revealed that the biosynthesized Ag NPs and commercial Ag NPs (ink nanosilver) were well dispersed and had a spherical shape. The size of biosynthesized Ag NPs is ranging from 5 to 37 nm with a mean diameter of 22.75 ± 10.88 nm, and the size of ink Ag NPs is ranging from 2 to 26 nm with a mean diameter of 16.523 ± 7.792 nm.

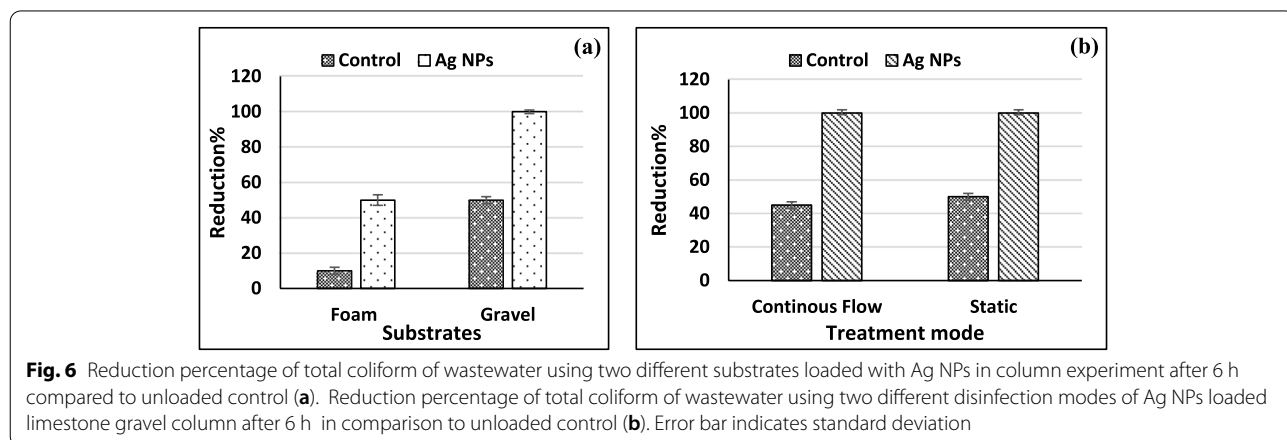
Wastewater disinfection experiments

It is worth noting that the used substrates have different binding capabilities to Ag NPs. The type of substrate controls the amount of Ag NPs that are loaded on it and thus controls the disinfection process. The concentration of Ag NPs remaining after coating was measured using atomic absorption, and thus, the remaining percentage was calculated. The remaining percentage was 8.8 and 21.2% after gravel and foam coating, respectively. Previous work by Pasricha et al. (2012) reported that cotton fabrics bind to Ag NPs more than wool and nylon. Reduction of total coliform count after column experiment using the two tested substrates loaded with and without Ag NPs is shown in Fig. 6a. The results revealed that after 6 h of exposure, the mean reduction percentage of the total coliform in control columns (without silver) was 50 and 10% in gravel and foam column, respectively. The mean reduction percentage of the total coliform count was 100% in the Ag NPs loaded gravel column, while 50% reduction was recorded in the Ag NPs foam column. Silver discharged from limestone gravel column was less than 0.01 mg/l which is below the standards to be discharged into the aquatic environment (Egyptian standards for liquid wastes discharging,

2015). This result may be due to that Ag NPs are stable and remain in zero-valent state (Pasricha et al. 2012).

Moustafa (2017) removes 98.5% of 41×10^5 CFU total coliform/100 ml after 24 h by foams that have been pre-soaked in 1118.6 mg/l Ag NPs. In his experiment, foams removed 50% of 25×10^5 CFU/ml after 6 h only, which may be due to the lower loaded Ag NPs and contacting time. Pal et al. (2022) coated Ag NPs on glass and polypropylene substrates; the efficiency against *E. coli* was 72.5% and 83.75% for coated glass and polypropylene, respectively. Limestone gravel is a highly porous substrate and is used in wastewater treatment processes (Fahim et al. 2019; El-Shahawy et al. 2020). Adsorption of bacteria to be disinfected depends on electrostatic attraction and charges of cell and particle surfaces (Stevik et al. 2004). Due to the higher efficiency of limestone than foam in binding and disinfection, limestone was chosen to test different disinfection conditions. As shown in Fig. 6b, the reduction percentage of the total coliform count was 100% after 6 h of using continuous flow mode or static mode. Continuous flow mode was performed at 2 ml/min; Mthombenia et al. (2012) also found that 2 ml/min was the most efficient flow rate.

The efficiency of the disinfection system depends on different parameters; one of them is the concentration of the disinfectant. The increased concentration of Ag NPs ensures the complete disinfection process (Mpenyana-Monyatsi et al. 2012; Moustafa 2017); on the other hand, it will certainly raise the cost and increase the discharged silver. Hence, using lower but efficient Ag NPs concentration to coat the substrate will reduce the cost. The results showed that after half an hour, the two tested concentrations (200 and 400 mg/l) eliminate about 50% of the initial total coliform count. With time passing, columns loaded with 400 mg/l concentration gradually reduce the count more than the one with 200 mg/l; however, both concentrations were eliminating the total coliform after 150 min (Fig. 7). Standard deviations of all tested times



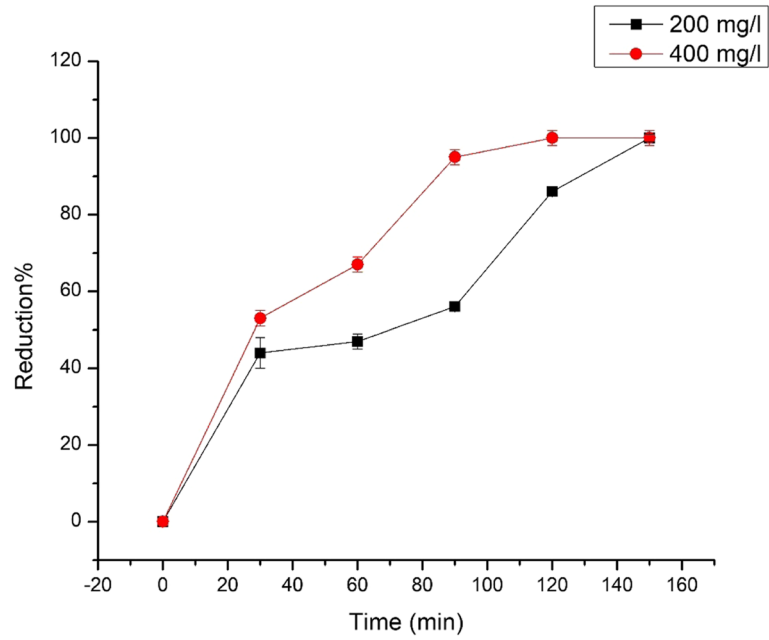


Fig. 7 Time course of the disinfection process using two different concentrations of biosynthesized Ag NPs, 200 and 400 mg/l

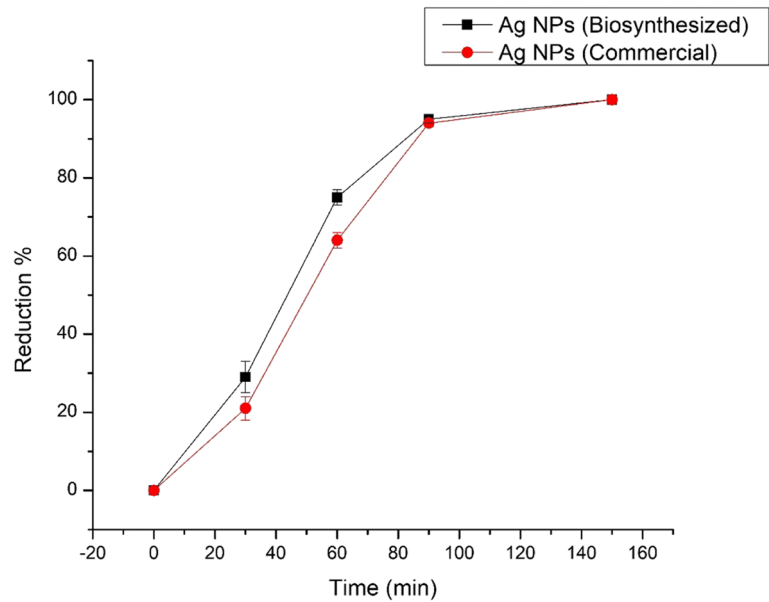


Fig. 8 The efficiency of the biosynthesized Ag NPs compared to commercial Ag NPs (ink nanosilver) in the disinfection process (the loaded concentration of each was 200 mg/l)

for both concentrations were from ± 1 to ± 3 . Depending on this results, gravel columns loaded with 200 mg/l of the biosynthesized Ag NPs were considered the more efficient option in the disinfection process.

The efficiency of Ag NPs in a certain field depends on their characteristics. The biosynthesis process produced heterogeneous Ag NPs suspension in both shape and size. The commercial Ag NPs were more homogenous in shape and size. The efficiency of both biosynthesized and commercial Ag NPs was determined. Standard deviations of all tested times for both Ag NPs were from ± 1 to ± 3 . After 90 min, there was no difference in reduction percentage, and both eliminate the total coliform bacteria after 150 min (Fig. 8).

Conclusions

In summary, a simple, non-toxic, and eco-friendly method was used to biosynthesis silver nanoparticles by *Streptomyces* sp. U13 (KP109813). The nanometrological characterization of biosynthesized Ag NPs and commercial Ag NPs (ink nanosilver) was studied for using them in wastewater disinfection. Two types of substrates, foam and limestone gravel, were selected to carry silver nanoparticles due to their high surface area. The type of substrate controls the amount of Ag NPs that are loaded on it and thus controls the disinfection process. Limestone gravel is a highly porous substrate and possesses higher efficiency of Ag NPs binding than foam. The results revealed that there was no significance between using biologically synthesized and commercially available Ag NPs for reducing bacterial contamination in wastewater. The concentration of 200 mg/l Ag NPs for coat limestone gravel with a contact time of 150 min is required to eliminate the coliform bacteria from wastewater.

Acknowledgements

Not applicable.

Authors' contributions

The authors read and approved the final manuscript. HT, screening, synthesis, and disinfection experiments and writing the manuscript; RS, characterizing Ag NPs, providing commercial ink Ag NPs and writing the manuscript; AL, synthesis, and disinfection experiments. HA, reviewing the manuscript and research team leader.

Funding

This study was funded by Science & Technology Development Fund (STDF) under Young Researcher Grant Agreement No 33466.

Availability of data and materials

The datasets used and/or analysed during the current study are available from the corresponding author on reasonable request.

Declarations

Ethics approval and consent to participate

Not applicable.

Consent for publication

Not applicable.

Competing interests

The authors declare that they have no competing interests.

Author details

¹Botany and Microbiology Department, Faculty of Science — Suez Canal University, Ismailia, Egypt. ²Nanometrology and Nanotechnology Laboratory, National Institute of Standards, Giza, Egypt.

Received: 30 April 2022 Accepted: 27 July 2022

Published online: 16 August 2022

References

- Abdulla HM, Taher HS, Ibrahim HA (2018) Bioleaching of uranium from Egyptian rocks using native actinomycete strains. *Geomicro. 35*(2). <https://doi.org/10.1080/01490451.2017.1288766>
- Abou-Dobara MI, El-Sayed A, Omar N (2017) *Streptomyces violaceoruber* ES: a producer of bioprospective metabolite for rapid and green synthesis of antibacterial silver nanoparticles. *Egypt J of Bot 57*(3):31–43. <https://doi.org/10.21608/ejbo.2017.1017.1089> https://ejbo.journals.ekb.eg/article_4085.html
- Al-Dhabi NA, Ghilan A, Esmail G, Arasu M, Veeramuthu DK, Ponnuragan K (2019) Environmental friendly synthesis of silver nanomaterials from the promising *Streptomyces parvus* strain Al-Dhabi-91 recovered from the Saudi Arabian marine regions for antimicrobial and antioxidant properties. *J Photochem Photobiol B Biol 197*:111529. <https://doi.org/10.1016/j.jphotobiol.2019.111529>
- Altintig E, Arabaci G, Altundag H (2016) Preparation and characterization of the antibacterial efficiency of silver loaded activated carbon from corncobs. *Surf Coat Technol 304*:63–67. <https://doi.org/10.1016/j.surfcoat.2016.06.077>
- Bakhtiari-Sardari A, Mashreghi M, Hossein E, Behnam-Rasouli F, Lashani E, Shahnavaz B (2020) Comparative evaluation of silver nanoparticles biosynthesis by two cold-tolerant *Streptomyces* strains and their biological activities. *Biotechnol Lett 42*:1985–1999. <https://doi.org/10.1007/s10529-020-02921-1>
- Benakashania F, Allafchianb A, Jalali S (2016) Biosynthesis of silver nanoparticles using *Capparis spinosa* L. leaf extract and their antibacterial activity. *Mod Sci 2*:251–258. <https://doi.org/10.1016/j.kijoms.2016.08.004>
- Bielefeldt AR, Kowalski K, Summers R (2009) Bacterial treatment effectiveness of point-of-use ceramic water filters. *Water Res 43*:3559–3565. <https://doi.org/10.1016/j.watres.2009.04.047>
- Bondarenko O, Juganson K, Ivask A, Kasemets K, Mortimer M, Kahru A (2013) Toxicity of Ag, CuO and ZnO nanoparticles to selected environmentally relevant test organisms and mammalian cells in vitro: a critical review. *Arch Toxicol 87*:1181–1200. <https://doi.org/10.1007/s00204-013-1079-4>
- Chu W, Hu J, Bond T, Gao N, Xu B, Yin D (2016) Water temperature significantly impacts the formation of iodinated haloacetamides during persulfate oxidation. *Water Res 98*:47–55. <https://doi.org/10.1016/j.watres.2016.04.002>
- Dada AO, Adekola F, Adeyemi O, Bello O, Oluwaseun A, Awakan O, Grace F (2018) Exploring the effect of operational factors and characterization imperative to the synthesis of silver nanoparticles. DOI. <https://doi.org/10.5772/intechopen.76947>
- Dubey SP, Lahtinen M, Sillanpaa M (2010) Tansy fruit mediated greener synthesis of silver and gold nanoparticles. *Process Biochem 45*:1065–1071. <https://doi.org/10.1016/j.procbio.2010.03.024>
- Duran N, Marcato P, De Conti R, Alves O, Costa F, Brocchi M (2010) Potential use of silver nanoparticles on pathogenic bacteria, their toxicity and possible mechanisms of action. *J Braz Chem Soc 21*:949–959
- Egyptian standards for liquid wastes discharging (2015) The Prime Minister Decree No. 967 for the year 2015, Guidelines for wastewater discharged into Egyptian aquatic environments.
- Elechiguerra JL, Burt J, Morones J, Camacho B, Gao X, Lara H, Yocaman M (2005) Interaction of silver nanoparticles with HIV-1. *J Nanobiotechnol*. <https://doi.org/10.1186/1477-3155-3-6>
- El-Shahawy A, El Moaty S, El-Shatoury S, Nafady A (2020) Performance assessment of stabilization ponds receiving wastewater of high organic load and feasibility of treatment using actinobacteria. *Desalin Water Treat 184*:292–305. <https://doi.org/10.5004/dwt.2020.25367>

- Erico RC, Noelia B, Tanya P, Gonzalo RS (2016) Green synthesis of silver nanoparticles by using leaf extracts from the endemic *Buddleja globosa* hope. *Green Chem Lett Rev* 10:250–256. <https://doi.org/10.1080/17518253.2017.1360400>
- Fahim R, Lu X, Jilani G, Hussain J, Hussain I (2019) Comparison of floating-bed wetland and gravel filter amended with limestone and sawdust for sewage treatment. *Environ Sci Pollut Res* 26:20400–20410. <https://doi.org/10.1007/s11356-019-05325-5>
- Fayaz AM, Balaji K, Girilal M, Yadav R, Kalaiichelvan P, Venketesan R (2010) Biogenic synthesis of silver nanoparticles and their synergistic effect with antibiotics: a study against gram-positive and gram-negative bacteria. *Nanomomed Nanotechnol Biol Med* 6:103–109. <https://doi.org/10.1016/j.nano.2009.04.006>
- Ferroudj N, Nzimoto J, Davidson A, Talbot D, Briot E, Dupuis V, Abramson S (2013) Maghemite nanoparticles and maghemite/silica nanocomposite microspheres as magnetic Fenton catalysts for the removal of water pollutants. *App Catal B: Environ* 136:9–18. <https://doi.org/10.1016/j.apcatb.2013.01.046>
- Gahlawat G., Choudhury A. R (2019) A review on the biosynthesis of metal and metal salt nanoparticles by microbes. *RSC Adv.* 9: 12944–12967. <https://doi.org/10.1039/C8RA10483B>
- Guzmán MG, Dille J, Godet S (2008) Synthesis of silver nanoparticles by chemical reduction method and their antibacterial activity. *Int J Miner Metall Mater* 2:91–98. <https://doi.org/10.7897/2230-8407.041024>
- Harajyoti M, Ahmed G (2011) Synthesis of silver nanoparticles and its adverse effect on seed germinations in *Oryzasativa*, *vignaradiata* and *Brassica campestris*. *Int J Adv Biotechnol Res* 2:404–413
- Jannathul FM, Lalitha P (2015) Biosynthesis of silver nanoparticles and its applications. *J of Nanotech* 1–19. <https://doi.org/10.1155/2015/829526>
- Kumari J, Mamta B, Ajeet S (2016) Characterization of silver nanoparticles synthesized using *Urticadioica* Linn. leaves and their synergistic effects with antibiotics. *J Radiat Res Appl Sci* 9:217–227. <https://doi.org/10.1016/j.jrras.2015.10.002>
- Li H, Jiang D, Huang Z, He K, Zeng G, Chen A, Yuan L, Peng M, Huang T, Chen G (2019) Preparation of silver-nanoparticle-loaded magnetic biochar/poly (dopamine) composite as catalyst for reduction of organic dyes. *J Colloid Interface Sci* 555:460–469. <https://doi.org/10.1016/j.jcis.2019.08.013>
- Lufsyi M, Edi S, Agung B, Kamsul A (2015) Optical properties of silver nanoparticles for surface plasmon resonance (SPR)-based biosensor applications. *J Mod Phys* 6:1071–1076. <https://doi.org/10.4236/jmp.2015.68111>
- Mahmood SN, Naeem S, Basit N, Usmani T (1993) Microbial evaluation of silver coated/impregnated sand for purification of contaminated water. *Environ Technol* 14:151–157. <https://doi.org/10.1080/09593339309385274>
- Matsumura Y, Yoshikata K, Kunisaki S, Tsuchido T (2003) Mode of bactericidal action of silver zeolite and its comparison with that of silver nitrate. *Appl Environ Microbiol* 69:4278–4281. <https://doi.org/10.1128/AEM.69.7.4278-4281.2003>
- Moustafa MT (2017) Removal of pathogenic bacteria from wastewater using silver nanoparticles synthesized by two fungal species. *Water. Science* 31(2). <https://doi.org/10.1016/j.wsj.2017.11.001>
- Mpenyana-Monyatsi L, Mthombeni N, Onyango M, Momba M (2012) Cost-effective filter materials coated with silver nanoparticles for the removal of pathogenic bacteria in groundwater international. *Int J Environ Res Public Health* 9:244–271. <https://doi.org/10.3390/ijerph9010244>
- Mthombeni NH, Mpenyana-Monyatsi L, Onyango M, Momba M (2012) Break-through analysis for water disinfection using silver nanoparticles coated resin beads in fixed-bed column. *J Hazard Mater* 217–218 133–140. <https://doi.org/10.1016/j.jhazmat.2012.03.004>
- Nangmenyi G, Yue Z, Mehrahi S, Mintz E, Economy J (2009) Synthesis and characterization of Ag nanoparticle impregnated fiberglass and utility in water disinfection. *Nanotech* 20:495–505. <https://doi.org/10.1088/0957-4484/20/49/495705>
- Pal S, Nisi R, Licciulli A (2022) Antibacterial activity of in situ generated silver nanoparticles in hybrid silica films. *Photochem* 2:479–488. <https://doi.org/10.3390/photochem2030033>
- Parisa G, Mozghan S, Masoud H, Farideh N, Susan A, Rosfarizan M, Amin B (2015) Sumac silver novel biodegradable nano composite for bio-medical application: antibacterial activity. *Molecules* 20:12946–12958. <https://doi.org/10.3390/molecules200712946>
- Pasricha A, Jangra S, Singh N, Dilbaghi N, Sood K, Arora K, Pasricha R (2012) Comparative study of leaching of silver nanoparticles from fabric and effective effluent treatment. *J Environ Sci* 24(5):852–859. [https://doi.org/10.1016/S1001-0742\(11\)60849-8](https://doi.org/10.1016/S1001-0742(11)60849-8)
- Phanjoy P, Ahmed G (2015) Biosynthesis of silver nanoparticles by *Aspergillus oryzae* (MTCC no. 1846) and its characterizations. *Nanosci Nanotechnol* 5(1):14–21. <https://doi.org/10.5923/j.nn.20150501.03>
- Preetha D, Prachi K, Chirom A, Arun R (2013) Synthesis and characterization of silver nanoparticles using cannonball leaves and their cytotoxic activity against MCF-7 cell line. *J Nanotechnol*:1–5. <https://doi.org/10.1155/2013/598328>
- Quang DV, Sarawade P, Hilonga A, Kim J, Chai Y, Kim S, Ryud J, Kim H (2011) Preparation of silver nanoparticle containing silica micro beads and investigation of their antibacterial activity. *Appl Surf Sci* 257:6963–6970. <https://doi.org/10.1016/j.apsusc.2011.03.041>
- Que ZG, Torres J, Vidal H, Rocha M, Pérez J, López I, Romero D, Reyna A, Sosa J, Pavón A, Hernández J (2018) silver nanoparticles - fabrication, characterization and applications. In: application of silver nanoparticles for water treatment. <https://doi.org/10.5772/intechopen.74675>
- Sathiya CK, Akilandeswari S (2014) Fabrication and characterization of silver nanoparticles using Delonix elata leaf broth. *Acta Part A: Mol Biomol. Spectrosc* 128:337–341. <https://doi.org/10.1016/j.saa.2014.02.172>
- Sathyavathi R, Krishna M, Rao S, Saritha R, Rao D (2010) Biosynthesis of silver nanoparticles using Coriandrum Sativum leaf extract and their application in nonlinear optics. *Adv Sci Lett* 3:1–6. <https://doi.org/10.1166/asl.2010.1099>
- Sayed R, Saad H, Hagagy N (2018) Silver nanoparticles: characterization and antibacterial properties. *Rend Fis Acc Lincei* 29:81–86. <https://doi.org/10.1007/s12210-017-0663-6>
- Selvi BCG, Madhavan J, Santhanam A (2016) Cytotoxic effect of silver nanoparticles synthesized from *Padina tetrastrumatica* on breast cancer cell line. *Adv Nat Sci: Nanosci Nanotechnol* 7:1–8. <https://doi.org/10.1088/2043-6262/7/3/035015>
- Stevik TK, Kari A, Ausland G, Hanssen JF (2004) Retention and removal of pathogenic bacteria in wastewater percolating through porous media: a review. *Water Res.* 38:1355–1367. <https://doi.org/10.1016/j.watres.2003.12.024>
- Sun Y, Chen Z, Wu G, Wu Q, Zhang F, Niu Z, Hu H (2016) Characteristics of water quality of municipal wastewater treatment plants in China: implications for resources utilization and management. *J Clean Prod* 131:1–9. <https://doi.org/10.1016/j.jclepro.2016.05.068>
- Tsibakhashvili NY, Kirkesali E, Pataraya D, Gurielidze M, Kalabegishvili T, Gvarjaladze D, Tsertsvadze G, Frontasyeva M, Zinicovska I, Wakstein M, Khakhanov S, Shvindina N, Shklover V (2011) Microbial synthesis of silver nanoparticles by *Streptomyces glaucus* and *Spirulina platensis*. *Adv Sci Lett* 4:1–10. <https://doi.org/10.1166/asl.2011.1915>
- Vasudeva RN, Suman B, Latha D, Soneya S, Sindhu G, Murali S, Venkata S, Saritha K, Vijaya T (2018) Biogenesis of silver nanoparticles using leaf extract of *Indigofera hirsuta* L. and their potential biomedical applications (3-in-1 system). *Artif Cells Nanomed Biotechnol* 1–11. <https://doi.org/10.1080/21691401.2018.1446967>
- Vidhyashree N, Yamini D, Lakshmi S (2015) Screening, isolation, identification, characterisation and applications of silver nanoparticles synthesized from marine actinomycetes (*Streptomyces grieseorubens*). *World J Pharm Res* 4(08):1801–1820
- Wagi S, Ahmed A (2020) Bacterial nanobiotic potential. *Green Process Synth* 9:203–211. <https://doi.org/10.1515/gps-2020-0021>
- Wang W, Huang G, Jimmy C, Wong P (2015) Advances in photocatalytic disinfection of bacteria: development of photocatalysts and mechanisms. *J Environ Sci* 34:232–247. <https://doi.org/10.1016/j.jes.2015.05.003>
- WHO (World Health Organization) (2015) Drinking-water: Fact sheet No. 391. <http://www.who.int/mediacentre/factsheets/fs391/en>

Publisher's Note

Springer Nature remains neutral with regard to jurisdictional claims in published maps and institutional affiliations.